

CREEP AND RELAXATION BEHAVIOR OF SPRING STEEL WIRES

Johannes Schleichert, Ulf Kletzin

Department of Mechanical Engineering, Institute for Design and Precision Engineering
Machine Elements Group, Technische Universität Ilmenau, Germany

ABSTRACT

This paper deals with creep and relaxation behavior of spring steel wires and helical compression springs. The mathematical description of this behavior over time regarding torsional stress is regarded closely. The derived equations based on the NORTON-BAILEY creep law are used for the evaluation of experimental data examining the relaxation as well as the creep behavior of different types of spring steel wire under torsional stress. As a part of the experimental approach, the heat treatments, which the wires were exposed to, as well as the level of relaxation stress and the surrounding temperature are varied. In this context the main influencing factors regarding creep deformations are discussed and creep specific characteristics are determined. Finally, the effect of different material, heat treatment, surrounding temperature and level of stress on the creep behavior are discussed and material constants identified.

Index Terms – spring steel wire, creep behavior, relaxation behavior

1. MOTIVATION AND GENERAL APPROACH

The reproducibility and accuracy of the machine element "spring" are seeing an increasing demand. During their life cycle springs are often times exposed to high amounts of mechanical stress and increased surrounding temperatures. This causes creep processes in the material, which can impair the function of the springs or even lead to their failure. The European standard EN 13906-1 provides a selection of relaxation figures which date back to 1960's, have largely unknown experimental conditions and are only valid for a relaxation time of 48 hours [1]. It is assumed that no significant creep deformations will take place after this amount of time, which is not entirely accurate. In order to predict these phenomena and to keep them as small as possible, the knowledge of how they can be mathematically engaged as well as carrying out experiments in which different influencing variables are varied and with whom creep-related material parameters can eventually be identified are required. For this purpose this paper aims to give a brief overview of the phenomenon "creep" and to present possibilities of its mathematical description. Subsequently results of creep and relaxation tests with spring steel wire and helical compression springs will be presented and the results discussed as well as interpreted with the provided mathematical relations.

2. BASIC KNOWLEDGE REGARDING CREEP PHENOMENONS

The phenomenon that solid materials are already beginning to show plastic deformations over time when being charged with stress conditions below the elastic limit is called "creep". The most important factor for creep processes besides the stress present in the material is the ambient temperature, which a sample or a component is exposed to. The reason therefor being

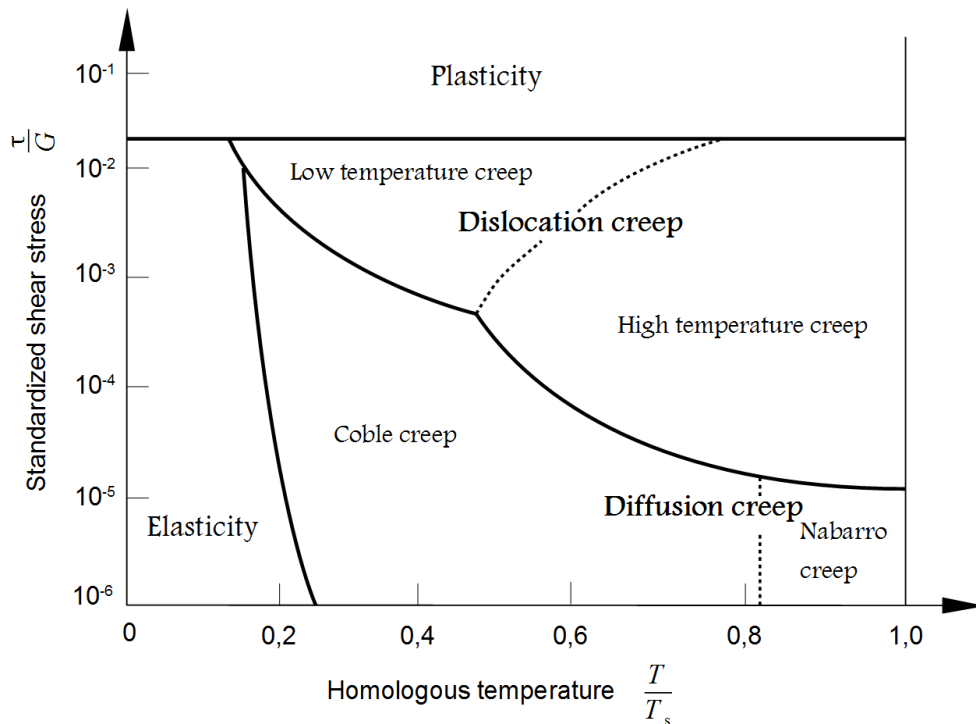


Figure 1:
Qualitative Deformation-Mechanism Map [2][3]

that creep processes are thermally activated space exchange events, whose extent is strongly temperature-dependent. Creep effects can be separated into three basic mechanisms [2]:

- Dislocation creep (Dislocations can avoid obstacles/blockages by climbing (attaching/sending out vacancies))
- Grain boundary sliding (Grains slipping of each other)
- Diffusion creep (Movement of vacancies in the material)

In the illustrated ASHBY diagram (**figure 1**), the shear stress at hand is normalized to the shear modulus and plotted against the ratio of the creep/relaxation temperature T to the melting temperature T_s . A temperature limit based on the melting temperature T_s frequently referred to in literature above which metallic materials begin to creep is $0,4 \cdot T_s$. While this can act as a sufficient guideline for many metals, some materials – including spring steel wires – show pronounced creep phenomena even at significantly lower temperatures [4]. Spring wire steels can thus be assigned to the low temperature creep, which is located in the area of the dislocation creep. The time course of creep processes is usually displayed with the aid of the resulting creep rate (strain rate) $\dot{\epsilon}$, which corresponds to the initial strain speed $\dot{\epsilon}_0$ at the beginning of the creep process. The course of the creep rate, as seen in **figure 2**, can be subdivided into three characteristic areas of varying duration and practical relevance [2][5]:

- Primary creep (the initially high creep rate steadily decreases as a result of strain hardening processes)
- Secondary creep (the creep rate reaches a minimum value, dynamic equilibrium between strain hardening and softening processes)
- Tertiary creep (the creep rate steadily increases until fracture due to irreversible impairment processes, hardly any significance in practice)

The shift of this so-called "creep curve" for higher temperatures towards greater amounts of strain rate is approximately the same behavior which can be observed with increasing stress.

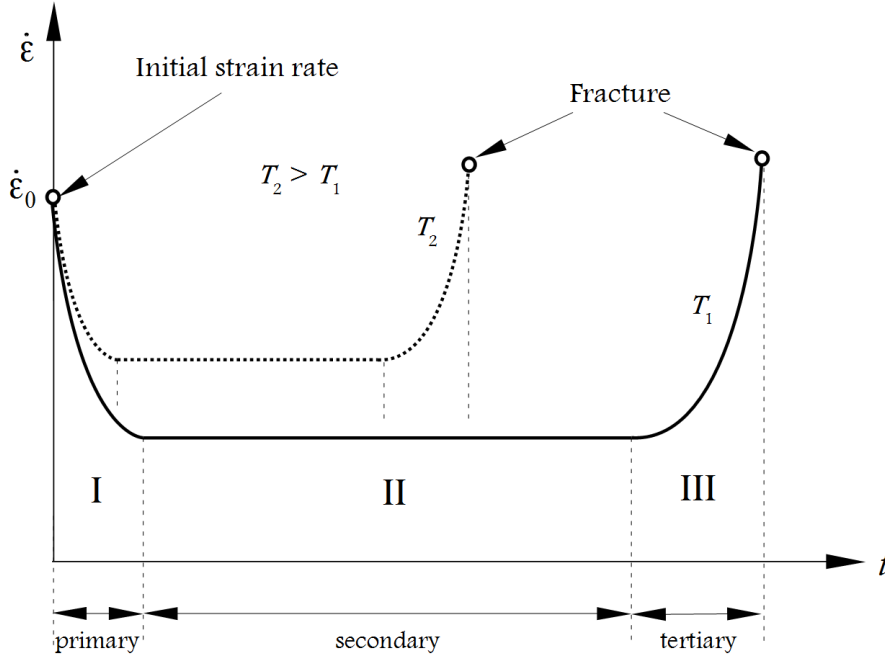


Figure 2:
Course of the strain rate (creep rate) over time regarding creep processes exposed to a constant level of stress [2]

The first key phase is the one of primary creep, which connects immediately to the elastic deformation. How quickly this area is giving way to the following, depends not only on the temperature, but also on the mechanical stress.

In practice, creep effects can manifest themselves in two different ways. On one hand, an increase in deformation can be observed while applying a constant external load. This phenomenon is referred to as "creep". If, on the other hand, a constant deformation is being implemented, the result is a reduction of the mechanical stress prevailing in the material respectively of the reaction forces/moments, which the component or the test body exerts on its contact elements. This phenomenon is referred to as "relaxation".

3. MATHEMATICAL APPROACH

There are a number of different approaches regarding the mathematical evaluation of creep effects. For torsional stress, which is the relevant stress situation when it comes to helical springs, the three most common ones were adapted by Prof. KOBELÉV in [6] and [7]. Based on this, the relations provided by the NORTON-BAILEY law, which is by far the most frequently used creep law, covering a large stress and temperature range, are used in this paper by applying them to the obtained experimental results. Creep processes occurring on wires loaded with torsional stress cause an increase of the twist of the wire – expressed via the torsion angle $\varphi(t)$ – over time, which can be described as [8]:

$$\varphi(t) = \frac{t^k}{k} \cdot l \cdot c_\tau \cdot \frac{2^{2m+3}}{d^{3m+4}} \cdot \left(\frac{M_t^0}{\pi} \cdot \frac{3m+4}{m+1} \right)^{m+1} \quad (1)$$

l represents the length of the twisted piece of wire, d the wire diameter and M_t^0 the temporally constant torsional moment, which loads the wire. m and k are creep related constants, which are dependent upon the material respectively the testing/practical conditions and have to be determined experimentally. k complies with the prevailing creep phase (**figure 2**) and reaches the value 1 in the secondary phase, whereas in the primary phase $0 < k < 1$ is valid. The variable m provides information on the creep mechanism at hand. In the case of diffusion creep, m equals 0, for grain boundary sliding $0 < m < 1$ holds true and regarding dislocation creep, m is

located between 3 and 6 (see **figure 1**) [5]. c_τ is an auxiliary parameter, which combines another three material-dependent creep constants while also being a function of m and k as well as taking the influence of the surrounding temperature T into account [8]:

$$c_\tau(k, m, T) = \frac{\bar{\gamma}}{\bar{t}^{k-1} \cdot \bar{\tau}^{m+1}} \cdot e^{\left(-\frac{Q_c}{R_c \cdot T}\right)} \quad (2)$$

The other variables in equation 2 are:

- $\bar{\gamma}$ – creep related strain parameter
- \bar{t} – creep related time parameter [s]
- $\bar{\tau}$ – creep related stress parameter [Pa]
- Q_c – activation energy of creep processes [J/mol]
- R_c – universal gas constant [1/mol K]
- T – absolute temperature [K]

When, on the other hand, considering relaxation processes, the over time decreasing torsional moment of the wire $M_t(t)$ needs to be described. Regarding torsional stress, the NORTON-BAILEY creep law delivers a hypergeometric function, which is dependent on the torsional moment before the start of the relaxation process M_t^0 [7]:

$$M_t(t) = {}_2F_1\left(\frac{1}{m}, \frac{4}{m}; \frac{4+m}{m}; -\frac{c_\tau \cdot G \cdot \tau_0^m \cdot m \cdot t^k}{k}\right) \cdot M_t^0 \quad (3)$$

G represents the shear modulus and τ_0 the maximum shear stress before the start of the relaxation process. For certain, fix values of m , this expression can be simplified into an elementary equation. Within the framework of the evaluated experiments, $m = 4$ has led to a good correlation between the experimental results and the mathematical model. The corresponding function, now independent of m , is [8]:

$$M_t(t) = M_t^0 \cdot \frac{k}{3} \cdot \frac{\left(1 + \frac{4 \cdot c_\tau \cdot G \cdot \tau_0^4 \cdot t^k}{k}\right)^{\frac{3}{4}} - 1}{c_\tau \cdot G \cdot \tau_0^4 \cdot t^k} \quad (4)$$

$m = 4$ is equivalent to the fact that the predominant creep mechanism is dislocation creep, which seems reasonable in view of **figure 1** considering the high levels of stress at hand. For helical compression springs, relaxation means that the spring is compressed by a fix spring deflection s and consequently the axial spring force $F(t)$, which the spring exerts on its contact area, decreases.

The spring force and the torsional moment loading the wire are directly proportional to one another and are idealized (which means without consideration of the unsymmetrical torsional stress distribution in the wire cross section of a helical compression spring, what can be argued to be justified considering all of the experiments are carried out with static load) linked via the following relation, as a function of the mean coil diameter D :

$$F(t) = \frac{2M_t(t)}{D} \quad (5)$$

Consequently, the correlations, which result for relaxation processes on helical compression springs with a constant wire diameter and constant mean coil diameter, take on a very similar form compared to those for wires under torsional stress. The general relation describing the

decrease of the spring force $F(t)$ over time as a function of the spring force at hand before the start of the relaxation process F_0 hence results in [5][6]:

$$F(t) = {}_2F_1\left(\frac{1}{m}, \frac{4}{m}; \frac{4+m}{m}; -\frac{c_\tau \cdot G \cdot \tau_0^m \cdot m \cdot t^k}{k}\right) \cdot F_0 \quad (6)$$

Correspondingly, for $m = 4$ [5][6]:

$$F(t) = F_0 \cdot \frac{k}{3} \cdot \frac{\left(1 + \frac{4 \cdot c_\tau \cdot G \cdot \tau_0^4 \cdot t^k}{k}\right)^{\frac{3}{4}} - 1}{c_\tau \cdot G \cdot \tau_0^4 \cdot t^k} \quad (7)$$

4. EXPERIMENTAL RESULTS

The experiments carried out consist of creep tests with spring steel wires, relaxation tests with spring steel wires and relaxation tests with helical compression springs. The majority of the tests were conducted with spring steel wires under torsional stress because of their considerably easier implementation while being very close to the actual stress situation of the component "spring". The results obtained from the tests on wires are opposed to the spring based relaxation tests and compared with each other.

4.1 Creep tests with spring steel wire

In the context of creep tests on wire, "creep" always means a further increase in the torsion angle $\varphi(t)$ beyond the angle that results from the preset amount of torsional stress, lying entirely within the elastic range – which means below the torsional yield point $\tau_{t,0.04}$. Within the scope of the experiment, the torsion angle has been continuously measured over time intervals ranging from 24 to 300 hours. For reasons of better visualization the subsequently shown curves are calculated curve fits based on the measuring points up to a creep time of 100 hours. The following types of spring steel wires with a wire diameter of 3mm have been part of the creep tests:

- Oil hardened and tempered spring steel wire, specifically VDSiCr
- Patented drawn spring steel wire, specifically lead bath drawn wire (Pb-patented)
- Stainless spring steel wire, specifically material no. 1.4310

Each of the wire types has been exposed to 2-3 well-established levels of heat treatments (HT) prior to the creep experiments, while the surrounding temperatures have been varied from 40°C up to 160°C (dependent on the temperatures that the correspondent springs will be exposed to in service and according to those mentioned in the European standards).

Figure 3 shows creep curves of the VDSiCr wire with a heat treatment of 350°C/30min for different levels of creep stress and creep temperature. The expected pattern of increasing creep deformation with growing amounts of creep stress as well as creep temperature presents itself quite clearly. While for small creep times and certain creep stress/temperature combinations the creep temperature is predominant regarding the induced creep deformation, it becomes clear that for creep times beyond 40h the creep deformation is mainly affected by the applied creep stress. Also, the slopes of the curves increase with the level of creep stress.

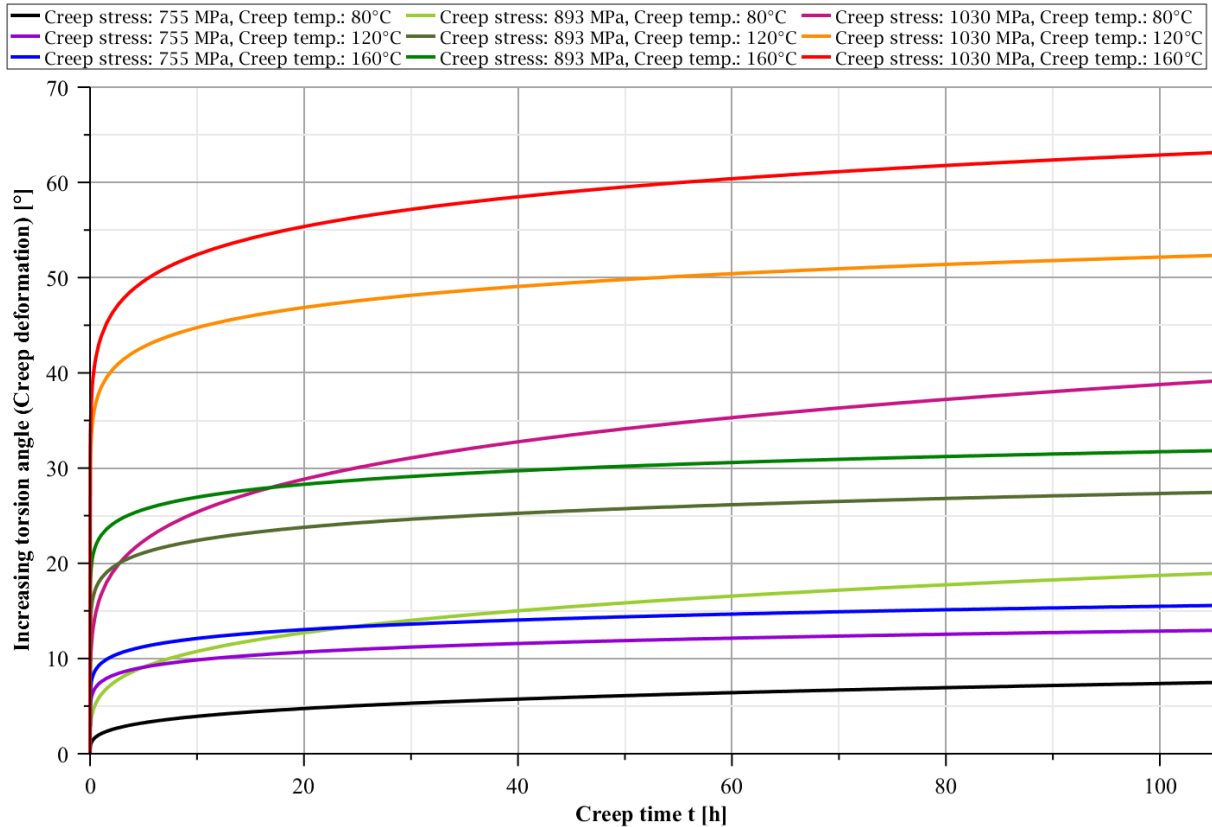


Figure 3: Creep curves of VDSiCr wire ($d=3\text{mm}$), $350^\circ\text{C}/30\text{min}$ heat-treated for various amounts of creep stress and temperature

Figure 4 opposes the two examined levels of heat treatment of the VDSiCr wire to one another for a fix value of creep stress (1030MPa) at various creep temperatures. It can generally be stated that the wires exposed to a heat treatment of $420^\circ\text{C}/30\text{min}$ tend to creep more than those with $350^\circ\text{C}/30\text{min}$. It is also striking that the $420^\circ\text{C}/30\text{min}$ -HT wire at a creep temperature of 80°C shows an even higher creep deformation than the $350^\circ\text{C}/30\text{min}$ -HT wire does at 120°C . The same applies to 120°C creep temperature relating to the $420^\circ\text{C}/30\text{min}$ -HT wire and 160°C creep temperature regarding the $350^\circ\text{C}/30\text{min}$ -HT wire. These dependencies correspond to the yield stress $\tau_{1,0,04}$ of the material after the heat treatment as shown in **table 1**.

In **figure 5** creep curves of the $200^\circ\text{C}/30\text{min}$ -HT Pb-patented wire are displayed for various amounts of creep stress and temperature. A similar picture as in the case of the VDSiCr wire is obtained, namely that the level of creep stress is highly dominant adverse the creep temperature in terms of an increase in creep deformation. For this type of wire material, even the initial range, in which – due to the flatter slope of the creep curves at lower creep temperatures –, regarding the VDSiCr wire, the effect of the creep temperature was slightly dominating for certain temperature/stress combinations, is no longer existent. This is most evidently demonstrated by the fact that a wire exposed to the creep stress/temperature combination of $755\text{MPa}/120^\circ\text{C}$ tends to creep slightly less than one exposed to $1030\text{MPa}/40^\circ\text{C}$. Furthermore, it can be observed that the creep conditions $755\text{MPa}/40^\circ\text{C}$ don't cause any more visible increase in creep deformation once a creep time of about 5h has passed.

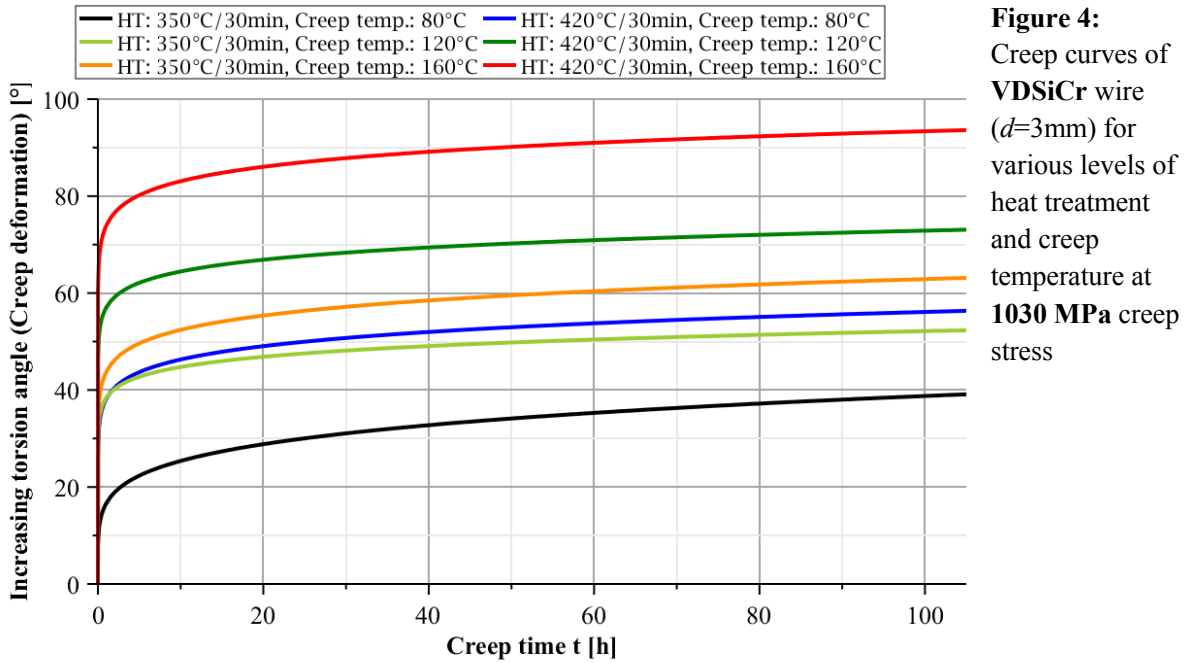


Figure 4: Creep curves of VDSiCr wire ($d=3\text{mm}$) for various levels of heat treatment and creep temperature at 1030 MPa creep stress

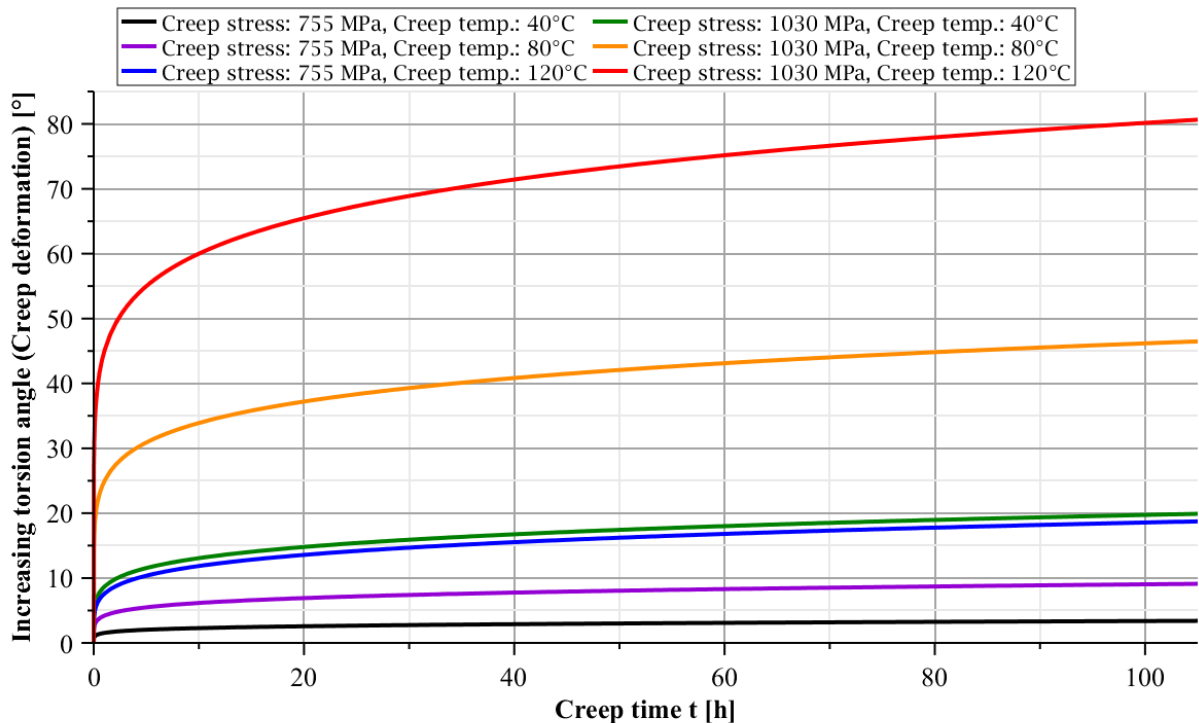


Figure 5: Creep curves of Pb-patented wire ($d=3\text{mm}$), 200°C/30min heat-treated for various amounts of creep stress and temperature

A comparison of the two tested levels of heat treatment concerning the Pb-patented wire at the various temperature levels considered in the course of the creep tests is given in **figure 6** in case of 1030MPa creep stress. What could be observed with the VDSiCr wire, can be stated here as well: the higher heat treatment temperature causes larger creep deformations. However, this phenomenon is considerably weaker in this case and has its maximum at a creep temperature of 80°C. While in terms of the VDSiCr wire, an analogy to the behavior of $\tau_{t,0.04}$ as to the level of heat treatment can be drawn, this doesn't hold true when it comes to the Pb-patented wire, since $\tau_{t,0.04}$ remains approximately constant at the transition of HT conditions from 200°C/30min to 250°C/30min (see **table 1**).

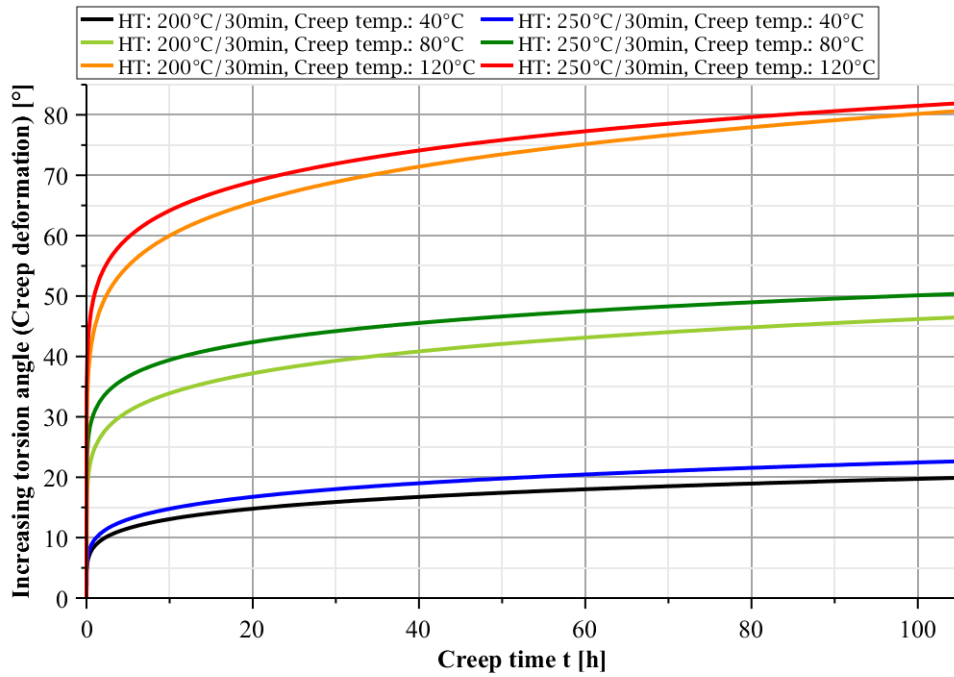


Figure 6: Creep curves of **Pb-patented** wire ($d=3\text{mm}$) for various levels of heat treatment and creep temperature at **1030 MPa** creep stress

Table 1 : $\tau_{t,0,04}$ -values [MPa] dedicated to types of spring steel wire for various levels of heat treatment

VDSiCr		Pb-patented		1.4310	
without HT	1008,4	without HT	647,8	without HT	501,8
350°C/30min	1103,4	200°C/30min	1069,4	200°C/30min	656,6
420°C/30min	1036,0	250°C/30min	1075,0	300°C/30min	692,6
				400°C/30min	712,0

A selection of creep curves concerning the last type of wire tested so far (1.4310) is shown for a HT of 300°C/30min in **figure 7** – again for several levels of creep temperature and stress, which in this case are smaller than those used for the other two wire materials considered so far due to the lower torsional yield points of 1.4310 (**table 1**). The creep deformation's hitherto noticed behavior as a function of its two principal influencing variables is anew confirmed and made clear once more by the fact that the creep conditions 549MPa/160°C result in smaller creep deformation than those consisting of 686MPa creep stress and 80°C creep temperature. **Figure 8** shows $\varphi(t)$ for the three different heat treatments of the 1.4310 wire, which have been investigated in the course of the creep tests, at 549MPa creep stress for two creep temperatures. Here we can again draw an analogy to the behavior of $\tau_{t,0,04}$, which increases for higher HT temperatures, while the creep deformation decreases significantly. Conversely, the dependence on the creep temperature rises massively towards lower HT temperatures. The 400°C/30min-HT wire barely shows an increase in creep deformation except for the always present initial build-up. Overall, the 1.4310 wire tends to creep much less than the other two examined types of wire.

This fact can be seen quite clearly in **figure 9**. All of the material/HT combinations for which creep tests have been carried out are displayed at a creep temperature of 120°C and at the maximum contemplated amount of creep stress (just below $\tau_{t,0,04}$ – in case of the 200°C/30min-HT 1.4310 wire even slightly above). Towards long creep times, the Pb-patented wire tends to creep the most, for creep times < 10h this holds true for the 420°C/30min-HT VDSiCr wire due to its large amount of initial creep deformation within the first hour. While the level of heat treatment has no significant influence on the creep curves

with regard to the Pb-patented wire, this is very much the case for the VDSiCr wire as well as for the 1.4310 wire at the transition from 200°C/30min HT to higher HT-temperatures.

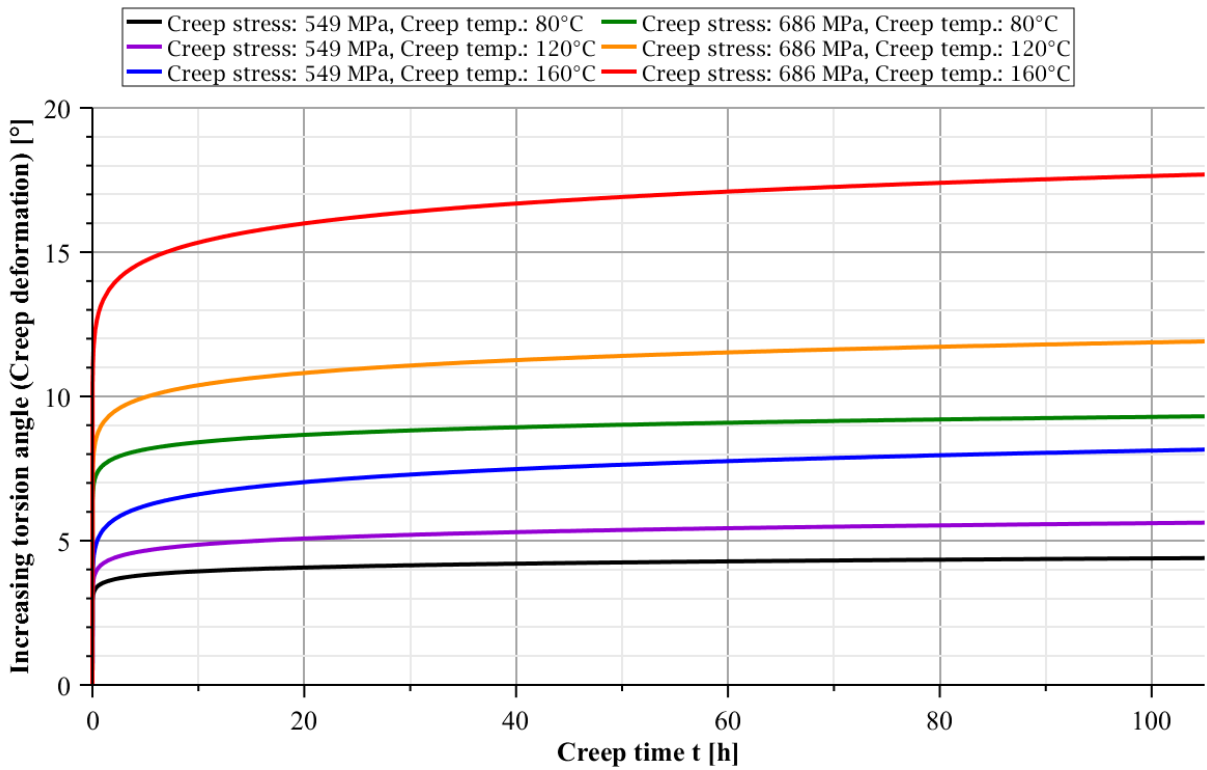


Figure 7: Creep curves of 1.4310 wire ($d=3\text{mm}$), 300°C/30min heat-treated for various amounts of creep stress and temperature

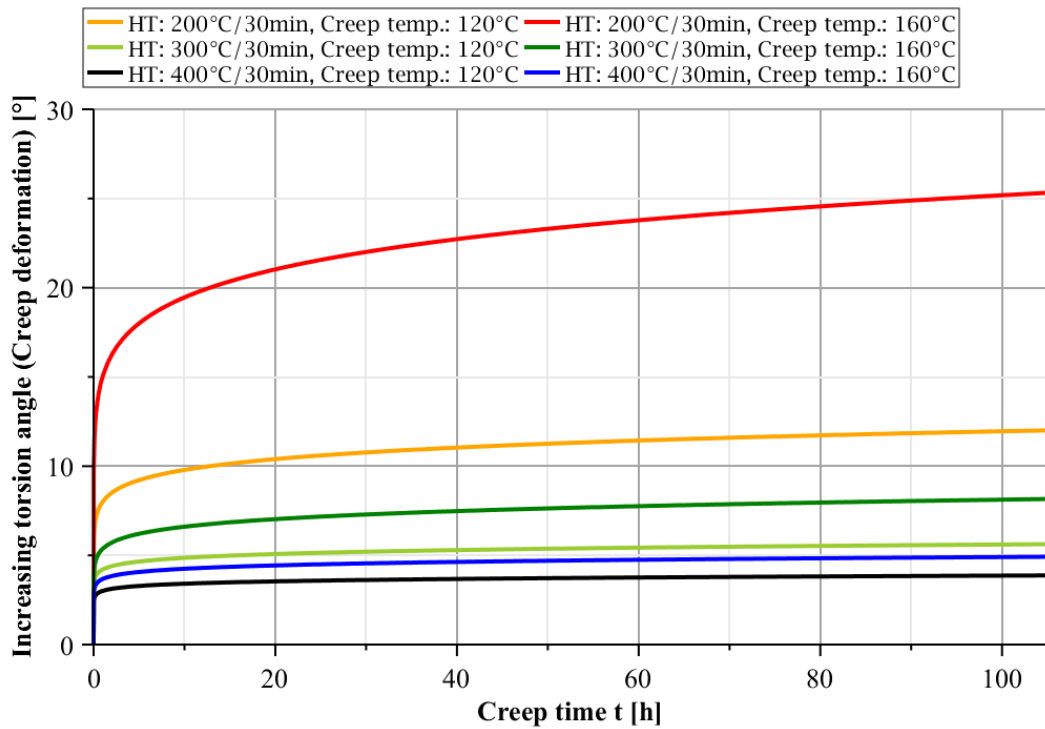


Figure 8: Creep curves of 1.4310 wire ($d=3\text{mm}$) for various levels of heat treatment and creep temperature at 549 MPa creep stress

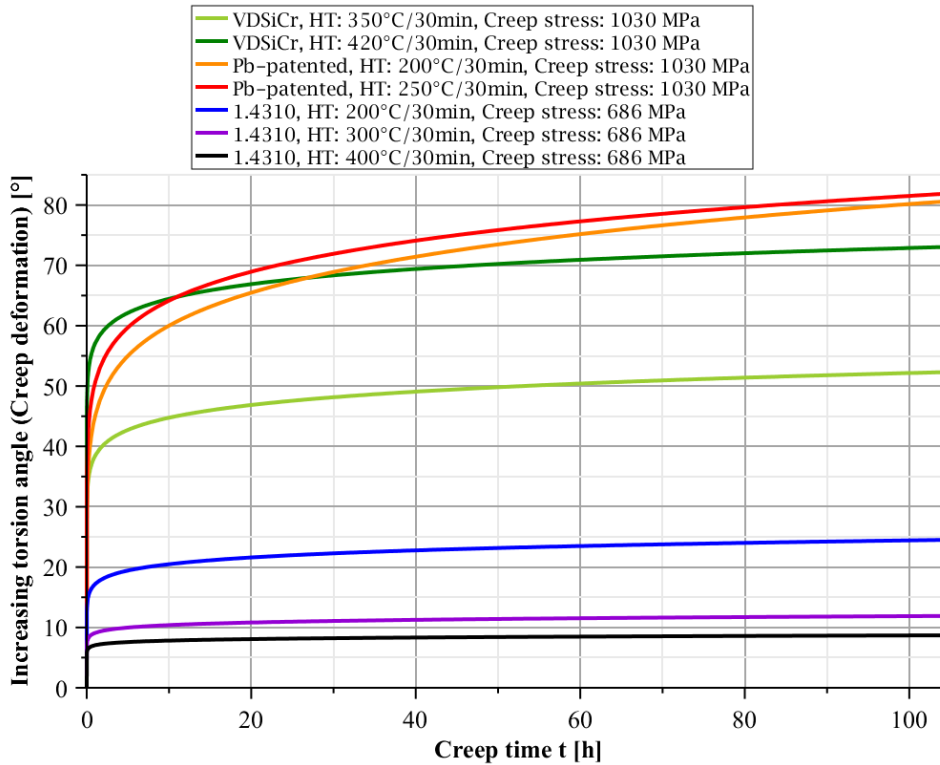


Figure 9: Creep curves of various types of spring steel wire ($d=3\text{mm}$) for various levels of heat treatment and creep stress at **120°C** creep temperature

4.2 Relaxation tests with spring steel wire

According to the European standard EN 13906-1 the relaxation is usually determined after 48h [1]. In the context of the relaxation experiments carried out, the decline of the torsional moment is determined as a function of time for test points in the interval 0 – 96h, more precisely at 0, 5, 24, 48 and 96h. The examined types of wire as well as their pre-treatments correspond to those of the creep tests.

The four temporal measuring points as well as the curve fits calculated by means of **equation 4** are displayed by plotting the moment ratio $M_t(t)/M_t^0$, which is precisely "1 – relaxation loss" over the relaxation time.

Figure 10 shows the relaxation curves of the VDSiCr wire for the two examined levels of heat treatment and various relaxation temperatures at 900MPa relaxation stress ($\approx 0,9 \cdot \tau_{t,0,04}$). At the same relaxation temperature, the 420°C/30min-HT wire exhibits greater relaxation losses than the 350°C/30min-HT wire, analog to what has been observed in the context of the creep tests. It's interesting how the non-heat-treated wire is integrated into the overall image, since it tends to relax less at a relaxation temperature of 80°C, at 120°C it's approximately the same, and only at 160°C a significantly greater deal of relaxation loss compared to the 420°C/30min-HT wire can be spotted (The $\tau_{t,0,04}$ value of the non-HT wire lies slightly below the one of the 420°C/30min-HT wire).

In **figure 11** the relaxation curves of the Pb-patented wire – with the respective heat treatments and relaxation temperatures at about $0,9 \cdot \tau_{t,0,04}$ relaxation stress – can be seen. Again, the circumstances determined within the scope of the creep tests are confirmed. Namely, that the 250°C/30min-HT wire suffers somewhat greater relaxation losses than the 200°C/30min-HT wire while being tested under otherwise identical conditions. Also shown are two curves of non-HT wires, which, due to their lower mechanical strength, could only be subjected to correspondingly less relaxation stress. Compared to the HT-wires, the non-HT wires show a considerably higher decrease of the moment ratio; at a relaxation temperature of 80°C the difference is particularly significant.

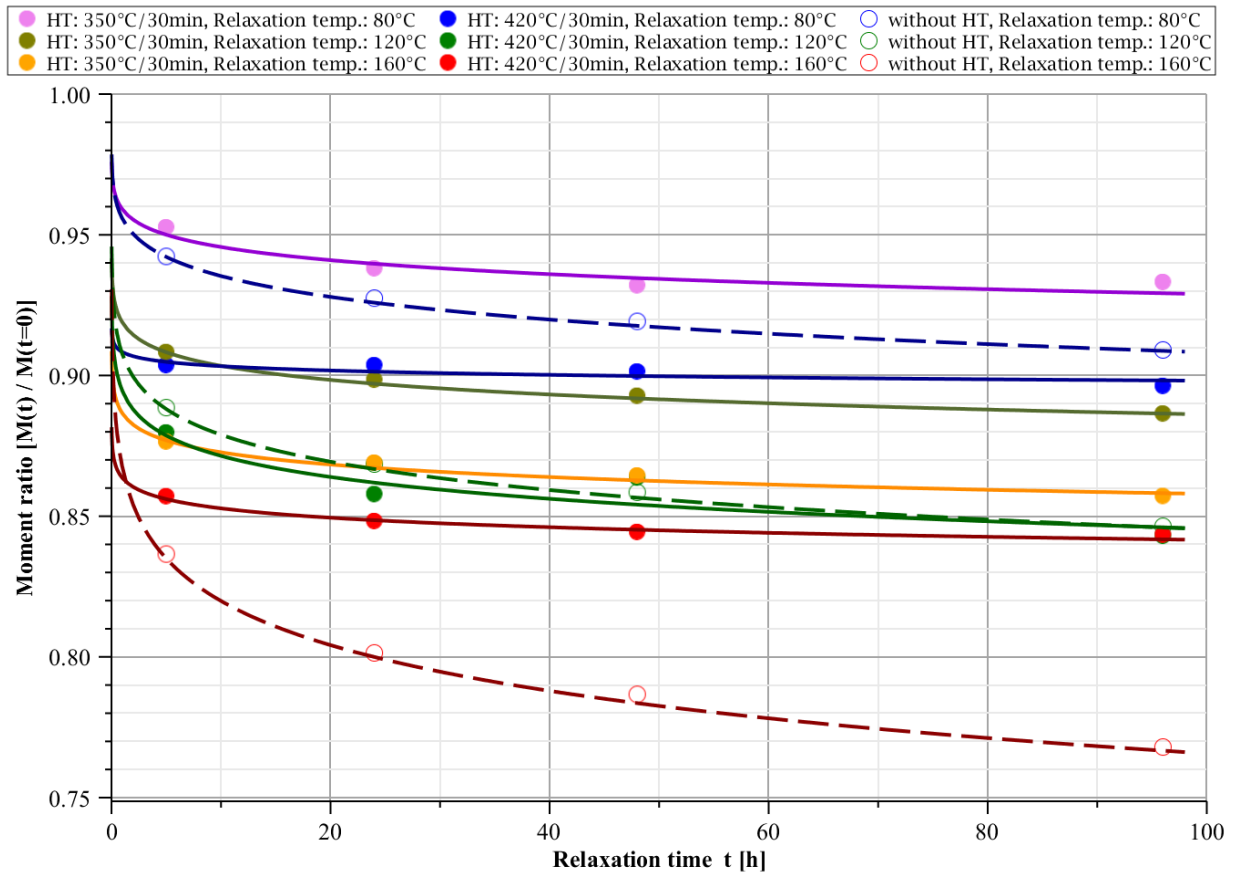


Figure 10: Relaxation curves of VDSiCr wire ($d=3\text{mm}$) for various levels of heat treatment and creep temperature at 900 MPa creep stress

Figure 12 summarizes some of the relaxation test results of the 1.4310 wire. The impact emanating from the heat treatment is clearly visible, after all, the $300^\circ\text{C}/30\text{min}$ heat-treated wires tend to relax considerably less than those with $200^\circ\text{C}/30\text{min}$ HT. This holds true for all plotted relaxation conditions.

Finally, **figure 13** gives a review of the relaxation curves of all the wire types considered at a relaxation temperature of 80°C respectively $0,9 \cdot \tau_{t,0,04}$ relaxation stress. As expected, the 1.4310 wires show the lowest and the non-HT Pb-patented wire the greatest relaxation loss. Considering long relaxation times, the $420^\circ\text{C}/30\text{min}$ -HT VDSiCr wire shares the same level of decreased moment ratio as both heat treatments of the Pb-patented wire.

4.3 Relaxation tests with helical compression springs

Analogous to the procedure for the relaxation tests with wires, test points were again determined in the interval from 0 – 96h, specifically at 0, 5, 24, 48 and 96h, only that in this case the decrease in the spring force has been measured. Relaxation tests with helical compression springs (HCS) have been carried out for springs made out of VDSiCr wire, spanning four spring indexes ($w = 3, 5, 8$ and 12), heat treatments analogous to the wire tests, relaxation temperatures and relaxation stresses. Once again, the four temporal measuring points as well as the curve fits calculated by means of **equation 7** are displayed over this relaxation time, in this context with the force ratio $F(t)/F_0$ (“1 – relaxation loss”) as ordinate.

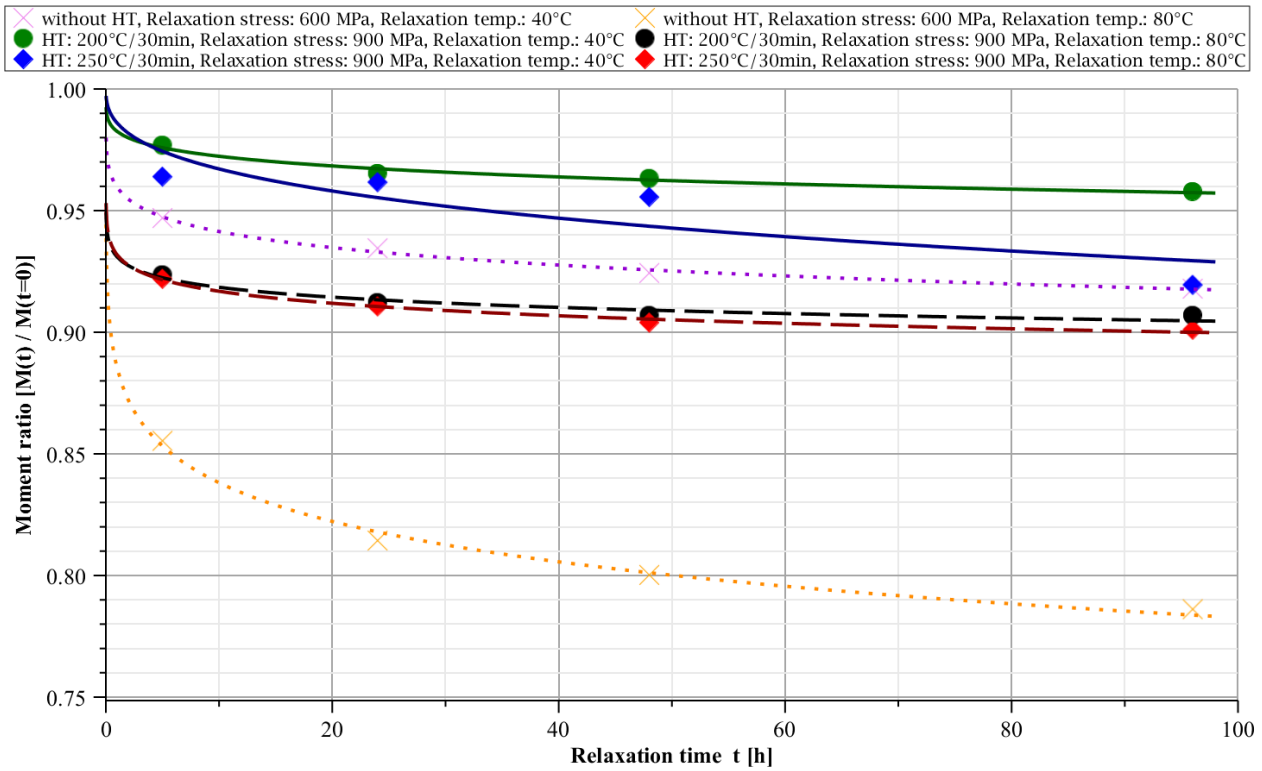


Figure 11: Relaxation curves of **Pb-patented** wire ($d=3\text{mm}$) for various levels of heat treatment and creep temperature at $0,9 \cdot \tau_{t,0,04}$ creep stress respectively

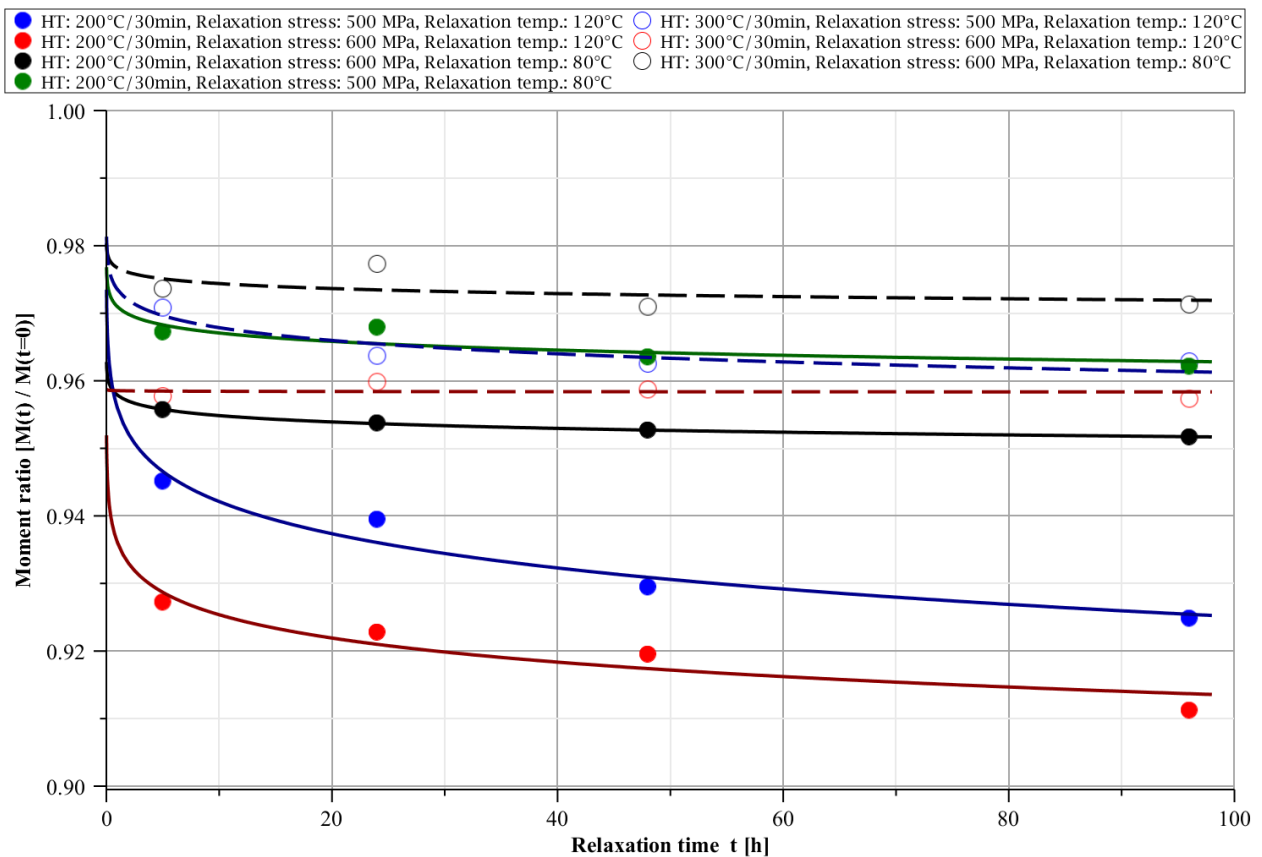


Figure 12: Relaxation curves of **1.4310** wire ($d=3\text{mm}$) for various levels of heat treatment, creep temperatures well as creep stress

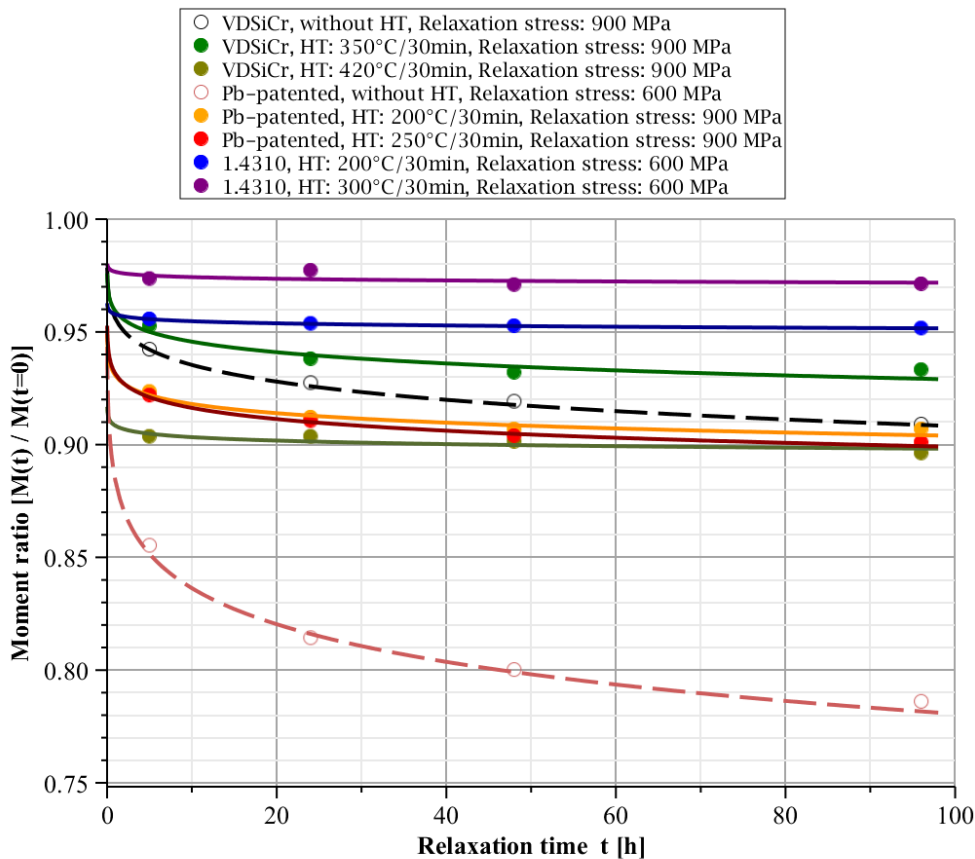


Figure 13: Relaxation curves of various types of spring steel wire ($d=3\text{mm}$) for various levels of heat treatment at 80°C creep temperature and $0,9*\tau_{t,0,04}$ creep stress respectively

Figure 14 shows HCS relaxation curves with respect to a spring index of $w = 12$ for the two examined heat treatments at various relaxation temperatures and 800MPa relaxation stress. It is apparent that, as expected, the $420^\circ\text{C}/30\text{min}$ HT results in greater relaxation losses compared to the $350^\circ\text{C}/30\text{min}$ HT, even when the displayed relaxation curves at 160°C relaxation temperature are pretty much identical for $t > 10\text{h}$. Generally, the magnitude of the relaxation losses is roughly comparable with those obtained by the tests with wire, although the springs were subjected to a lower amount of relaxation stress. In order to make more precise statements on this subject, further test results are required. The generated measuring points also occasionally show a clear outlier, which can, among other things, be attributed to the more complex geometry of springs as opposed to wires, which makes the ideal case of completely identical test objects nearly impossible.

Finally, in **figure 15** relaxation curves of HCS made of $350^\circ\text{C}/30\text{min}$ -HT VDSiCr wire can be seen for all four spring indexes at a relaxation temperature of 120°C and 800MPa relaxation stress. $w = 3$ and $w = 12$ show the greatest relaxation losses, while $w = 5$ and $w = 8$ are nearly coincident and tend to relax less than the springs with the very large or very small spring index. However, all four curves are located relatively close together and were determined at a comparatively low level of relaxation stress.

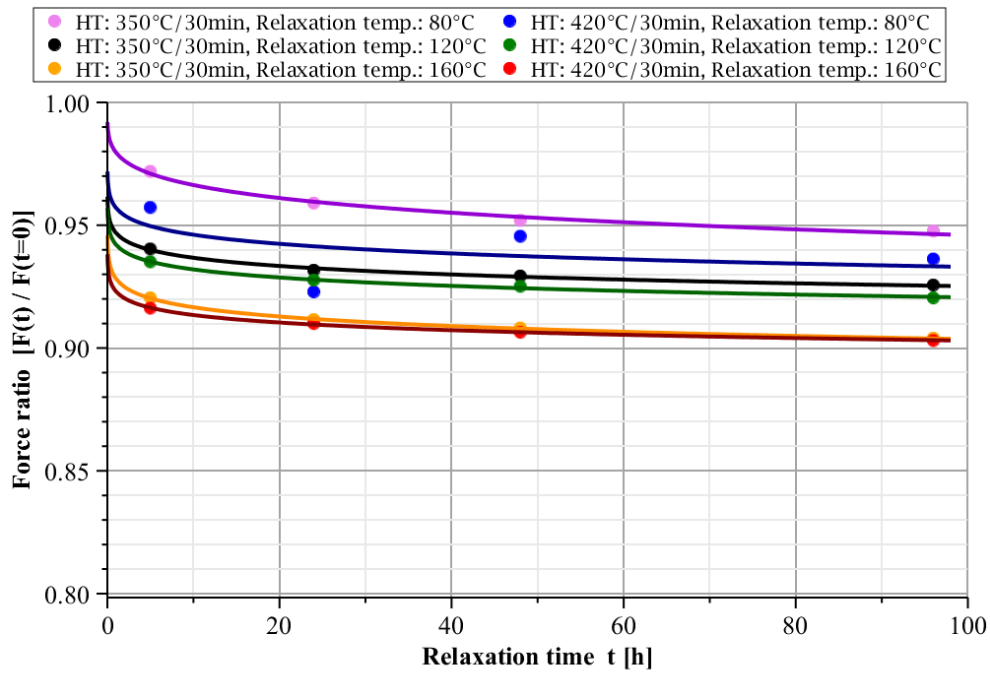


Figure 14: Relaxation curves of **non-preset** helical compression springs made of **VDSiCr** wire ($d=3\text{mm}$) with $w = 12$ for various levels of heat treatment and relaxation temperature at **800 MPa** relaxation stress

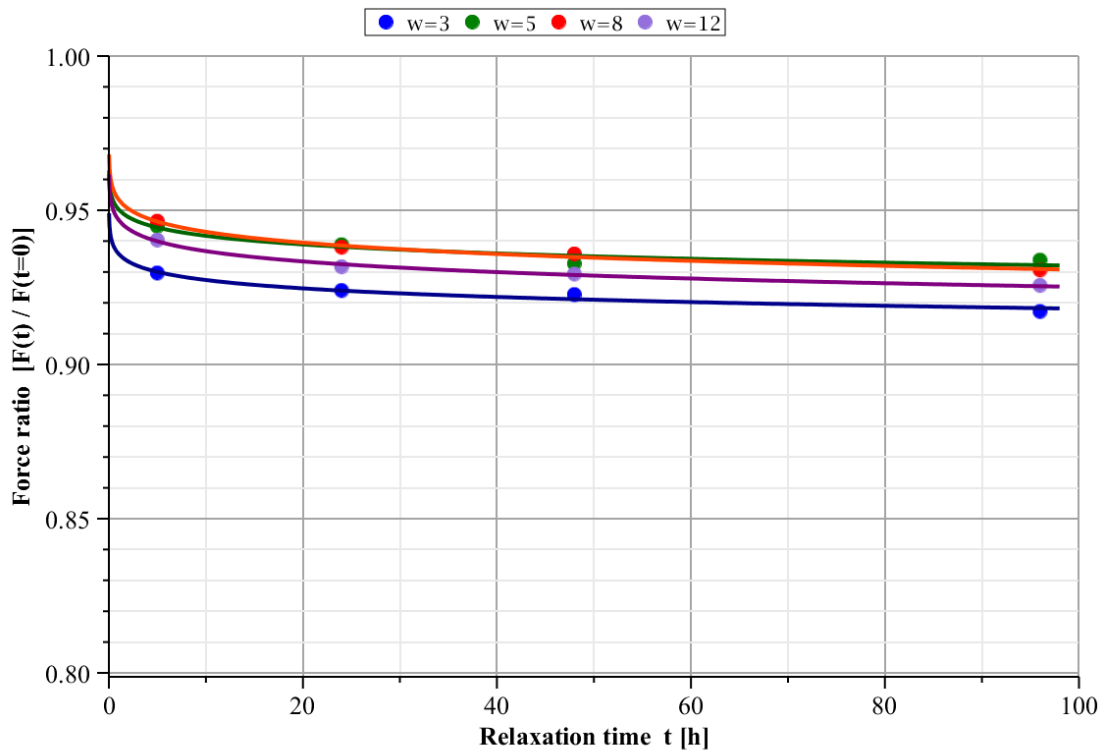


Figure 15: Relaxation curves of **non-preset** helical compression springs made of **VDSiCr** wire ($d=3\text{mm}$), **350°C/30min** heat-treated for various spring indexes at a relaxation temperature of **120°C** and **800 MPa** relaxation stress

5. CREEP SPECIFIC CHARACTERISTICS AND MATERIAL CONSTANTS

Concluding, in this section, the experimental results of the creep tests with spring steel wire are being used to determine creep specific characteristics and material constants. The measured values of the increasing torsion angle $\varphi(t)$ are imported in MAPLE and evaluated with respect to the three unknown creep parameters k , m and c_τ by means of the corresponding relation of the NORTON-BAILEY creep law (**equation 1**) via a non-linear curve fit based on the least-squares method.

m approximately adopts the value 4 for all creep conditions. In **figures 16 to 19** the two remaining creep parameters k and c_τ are plotted against the creep stress respectively the creep temperature for different values of the respective other. According to this, k decreases with increasing creep temperature. The exception is the 1.4310 wire with all heat treatments, for which k increases (**figure 16**). It can generally be stated that k is significantly smaller than 1 at all times, hence all the creep tests carried out can be assigned to the primary creep phase (see **figure 2**). Also, k decreases with increasing creep stress – here, this holds also true for the 1.4310 wire (**figure 17**). c_τ increases with increasing creep temperature for all examined types of wire and their respective heat treatments (**figure 18**) while remaining approximately constant as a function of creep stress. Here too, the 1.4310 wire represents the exception, for which c_τ decreases with increasing stress (**figure 19**). It is worth noting that c_τ itself is a function of m as well as k and, what is more, includes the influence of the creep temperature via the mathematical approach (see **equation 2**).

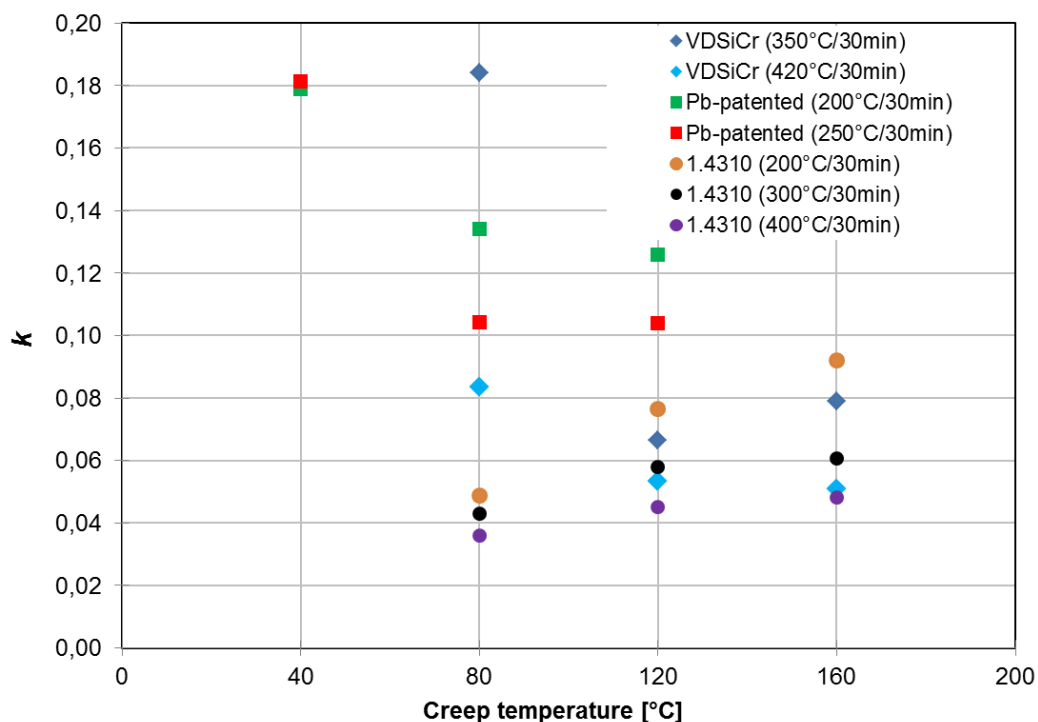


Figure 16: Creep parameter k as a function of creep temperature for various types of spring steel wire and respective levels of heat treatment

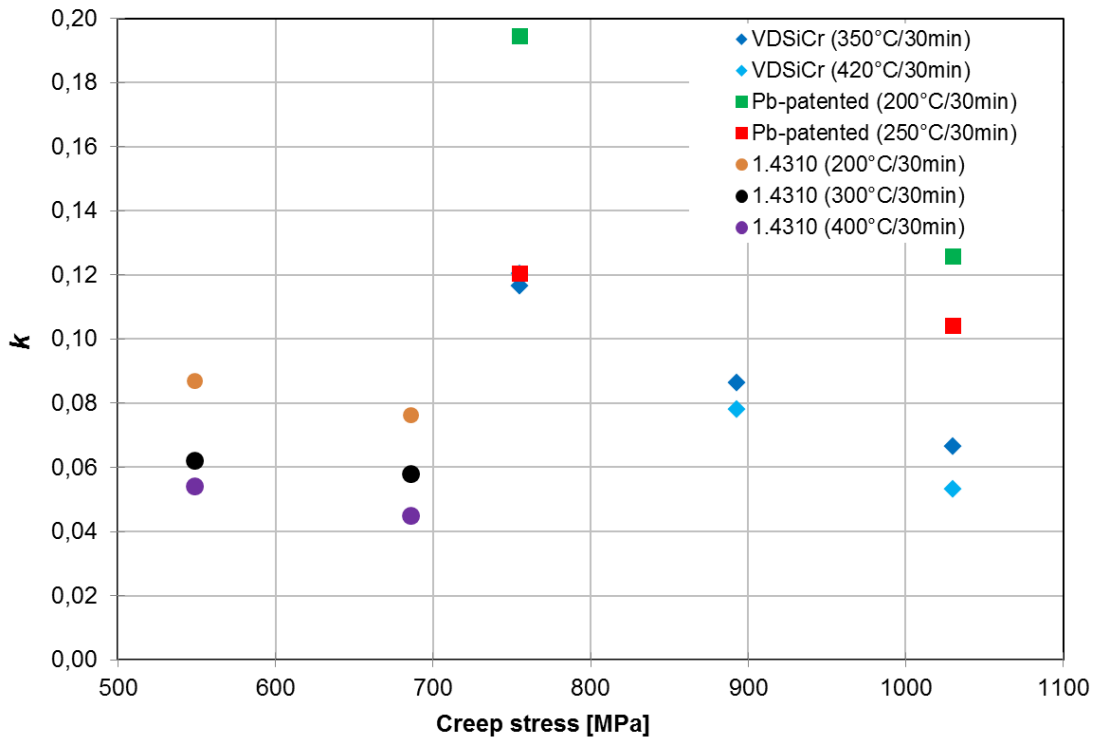


Figure 17: Creep parameter k as a function of creep stress for various types of spring steel wire and respective levels of heat treatment

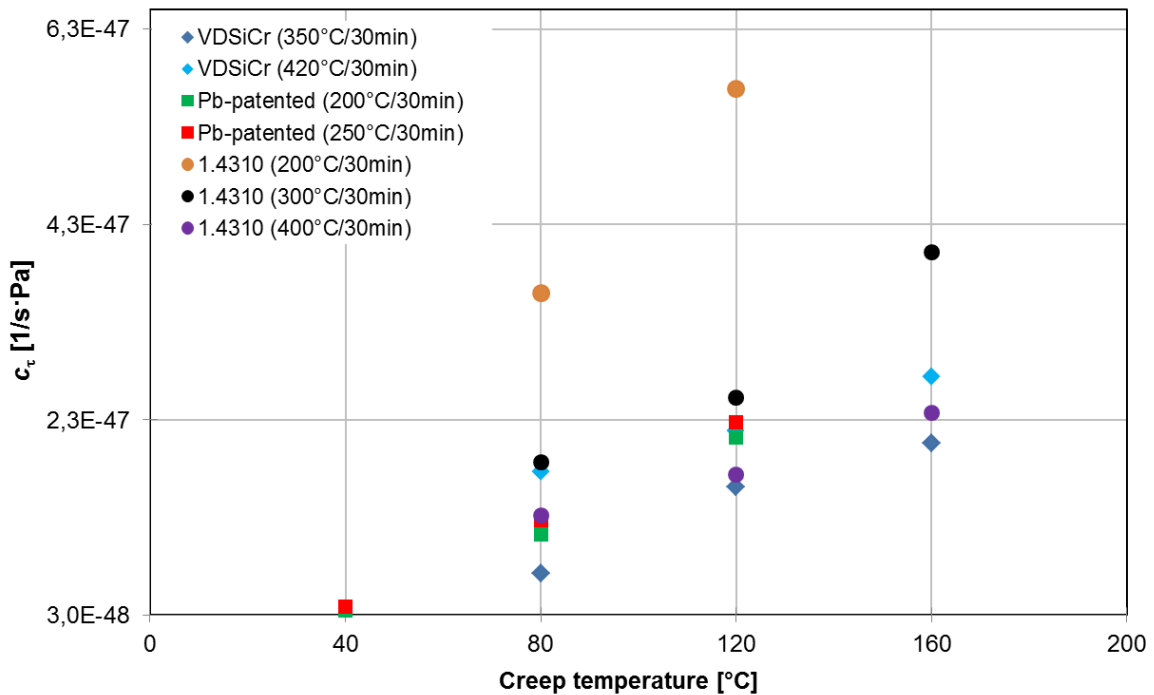


Figure 18: Creep parameter c_τ as a function of creep temperature for various types of spring steel wire and respective levels of heat treatment

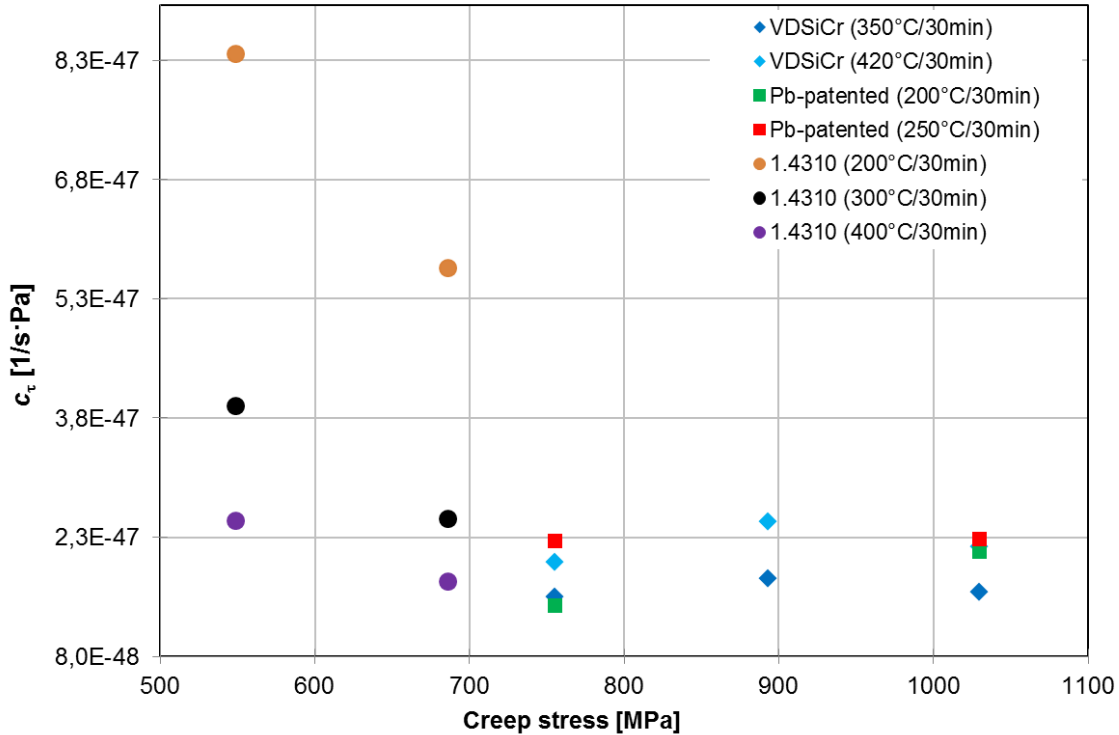


Figure 19: Creep parameter c_τ as a function of creep stress for various types of spring steel wire and respective levels of heat treatment

6. CONCLUSION AND OUTLOOK

The experimental examinations have shown that the NORTON-BAILEY creep law is well suited to represent the creep and relaxation behavior of spring steel wires and helical compression springs satisfyingly. The resulting creep parameters suggest the creep mechanism at hand to be dislocation creep ($m = 4$) and locate all creep processes up to 300h of creep time in the primary creep phase ($k < 1$). As expected, the creep and relaxation losses increase with increasing amounts of creep, respectively relaxation, stress and temperature. With regard to the effect of heat treatment, it can generally be stated that heat treatment has a positive effect on the creep/relaxation behavior of spring steel wires, respectively helical compression springs made therefrom. As far as the individual types of wire are concerned, it has been found that the 420°C/30min HT leads to considerably greater creep/relaxation losses than the 350°C/30min HT in case of the VDSiCr wire. As for the Pb-patented wire, the two respective heat treatments are approximately at the same creep/relaxation level, even though the 250°C/30min HT results in slightly more pronounced creep/relaxation processes. In case of the examined 1.4310 wire, the creep/relaxation losses decrease continuously with increasing temperature during the heat treatment: the 200°C/30min HT leads to the most distinct creep/relaxation processes, the 400°C/30min HT to the least. The comparison of the three materials, which have been part of the experiments, shows that the 1.4310 wire tends to creep/relax least and the Pb-patented wire strongest, when it comes to long creep/relaxation times (with respect to levels of creep stress of $\approx 0,9 \cdot \tau_{t0,04}$ and otherwise identical testing conditions).

As a next step and based on the hitherto gained insights, relaxation tests on pre-set helical compression springs are to be carried out, since the manufacturing step “pre-setting” is specifically conducted to anticipate relaxation processes in service. This deliberate application of stress within the plastic range is being realized for wires too by exposing them to a corre-

spondingly large amount of pre-torsion stress ahead of the actual creep/relaxation tests. Experiments on other wire diameters ($d = 2\text{mm}$ and $d = 6\text{mm}$) seem reasonable to perform as well, considering the fact, that the wire diameter is represented with double-digit power in the descriptive equations provided by the NORTON-BAILEY creep law. In conjunction to these, the aim is to split up the summary creep constant c_τ into their individual components in order to be finally able to comprehend creep and relaxation behavior more accurately.

REFERENCES

- [1] DIN EN 13906-1: Cylindrical helical springs made from round wire and bar – Calculation and design – Part 1: Compression springs, November 2013
- [2] J. Rösler, H. Harders and M. Bäker, Mechanisches Verhalten der Werkstoffe, 4., revised and extended run, Springer Vieweg, Wiesbaden, 2013
- [3] M.F. Ashby and H.J. Frost: Deformation-Mechanism Maps – The Plasticity and Creep of Metals and Ceramics, URL: <http://engineering.dartmouth.edu/defmech/>, access date: 20.06.2017
- [4] G.B. Graves and M. O'Malley, "Relaxation bei Schraubendruckfedern", Draht 34 – Nr. 3, pp. 109–112, 1983
- [5] V. Kobelev, "Mathematisches Modell für das Kriechen und Relaxation von Federn", Ilmenauer Federntag, Forschungsgruppe Draht und Federn der TU Ilmenau, Ilmenau, 2015
- [6] V. Kobelev, "Relaxation and creep in twist and flexure", Multidiscipline Modeling in Materials and Structures 10 – Nr. 3, pp. 304–323, October 2014
- [7] V. Kobelev, "Some basic solutions for nonlinear creep", International Journal of Solids and Structures 51 – Nr. 4, pp. 3372–3381, 2014
- [8] J. Schleichert, "Kriech- und Relaxationsverhalten von Federstahldrähten und Schraubendruckfedern", Technische Universität Ilmenau, Master Thesis, 2016

CONTACTS

M. Sc. Johannes Schleichert
Prof. Dr.-Ing. Ulf Kletzin

johannes.schleichert@tu-ilmenau.de
ulf.kletzin@tu-ilmenau.de